DYNAMICS OF BRAIN ACTIVITY CAPTURED BY GRAPH SIGNAL PROCESSING OF NEUROIMAGING DATA TO PREDICT HUMAN BEHAVIOUR

Thomas A.W. Bolton[⋆†] *Dimitri Van De Ville*[⋆†]

[⋆] Institute of Bioengineering, École Polytechnique Fédérale de Lausanne, Switzerland
[†] Department of Radiology and Medical Informatics, University of Geneva, Switzerland

ABSTRACT

Joint structural and functional modelling of the brain based on multimodal imaging increasingly show potential in elucidating the underpinnings of human cognition. In the graph signal processing (GSP) approach for neuroimaging, brain activity patterns are viewed as graph signals expressed on the structural brain graph built from anatomical connectivity. The energy fraction between functional signals that are in line with structure (termed *alignment*) and those that are not (*liberality*), has been linked to behaviour. Here, we examine whether there is also information of interest at the level of temporal fluctuations of alignment and liberality. We consider the prediction of an array of behavioural scores, and show that in many cases, a dynamic characterisation yields additional significant insight.

***Index Terms*—** Graph signal processing, alignment, liberality, dynamic functional connectivity, behaviour

1. INTRODUCTION

Magnetic resonance imaging (MRI)-based approaches have enabled the quantification of anatomical wiring between remote brain areas, and the resulting structural connectome is governed by precise organisational rules, in which regions are clustered into modules linked by a group of densely interconnected hubs [1]. On top of this structural scaffold, combined with local nonlinear processing, complex spatio-temporal activity is expressed that can be captured by functional MRI (fMRI) during task and resting-state [2].

A recently introduced analytical avenue has been to study brain structure and function in conjunction: this way, confounding factors that impede the functional signals, such as physiology- or motion-driven signal changes [3], may be damped out by a structure-informed analysis. Meanwhile, functional brain features of truly neural relevance would be associated to a structural counterpart.

Recently, whole-brain functional connectivity maps and grey matter density were analysed jointly at the voxel level through deep learning to establish their joint predicting potential in the context of schizophrenia [4]. At the coarser scale of a regional brain parcellation, structural connectivity information was also used to inform the total variation-based deconvolution of fMRI data [5].

Another well-suited analytical approach is graph signal processing (GSP) [6], in which a structural graph $\mathcal{G}$ that describes anatomical connectivity between brain regions is constructed, and the functional activation pattern $\mathbf{x}_t$ at a given time point t is treated as a signal on $\mathcal{G}$. In the context of an attention switching task, [7, 8] showed an association between switch cost and *liberality* of the functional signals with respect to the underlying anatomical scaffold. In a subsequent work, [9] also observed that the balance between functional *alignment* (the energy fraction of the functional signals that is in line with structure) and liberality follows a gradient along the cortical surface that also distinguishes lower-order sensory functions from higher-order cognitive ones.

Since alignment and liberality have so far been quantified as temporal averages over a full scanning session, the now well acknowledged dynamics of functional brain reconfigurations (see [10] for a comprehensive review) is not captured. Here, we explore whether a dynamic GSP characterisation provides additional information to predict an array of behaviourally relevant scores.

2. MATERIALS AND METHODS

2.1. Data preprocessing

We considered structural, functional and behavioural data acquired within the scope of the *Human Connectome Project* (HCP) [11]. Diffusion-weighted imaging data from 56 unrelated subjects was processed with the *MRtrix* toolbox [12] (multi-shell multi-tissue response function estimation, spherical deconvolution, tractogram generation with 10^7 output streamlines between $R = 360$ regions from the Glasser atlas [13]), and averaged to yield a common graph representation $\mathcal{G} = (\mathcal{V}, \mathbf{A})$ of the data, with $\mathcal{V}$ the set of nodes (brain regions) and $\mathbf{A} \in \mathbb{R}^{R \times R}$ the adjacency matrix summarising average physical wiring between them across subjects.

We analysed minimally preprocessed resting-state fMRI data of 181 subjects (LR acquisition session, 15 min of recordings at a TR of 0.72 s), which had already underwent realignment, co-registration and warping to Montreal Neuro-

logical Institute space. We discarded the first ten volumes, and performed linear detrending of voxel-wise time courses, regression of low-frequency DCT basis functions (frequency cutoff: 0.01 Hz), atlasing [13], and scrubbing at a framewise displacement threshold of 0.3 mm with cubic spline interpolation to re-estimate excised volumes.

We initially considered the behavioural scores of 951 subjects for whom less than 5% of entries were missing, and used probabilistic PCA to fill in missing values while deriving 62 summarising measures across anthropometric, cognitive and psychometric domains. We performed z-scoring for each domain measure, and sampled the scores linked to the 181 subjects for which functional data was preprocessed.

2.2. Graph signal processing analyses

Let the adjacency matrix $\mathbf{A}$ and the subject-specific regional activation time courses $\mathbf{X} \in \mathbb{R}^{R \times T}$, with $R = 360$ regions and $T = 1190$ time points. The symmetric adjacency matrix can undergo an eigendecomposition as $\mathbf{A} = \mathbf{V}\mathbf{\Lambda}\mathbf{V}^\top$, with $\mathbf{V} = [\mathbf{v}_1|\mathbf{v}_2|...\mathbf{v}_R]$ containing the *eigenmodes* (spatial frequencies on the graph), arranged in descending eigenvalue order. Because $\lambda_k = \mathbf{v}_k^\top \mathbf{A}\mathbf{v}_k = \sum_{i \neq j} A_{i,j}[\mathbf{v}_k]_i[\mathbf{v}_k]_j$, larger eigenvalues are associated to lower frequencies on the graph.

Each functional signal time point $\mathbf{x}_t$ lives on $\mathcal{G}$, and can be expressed as a linear combination of the graph's constituting eigenmodes [6]:

$$\mathbf{x}_t = \mathbf{V}\tilde{\mathbf{x}}_t, \tag{1}$$

where $\tilde{\mathbf{x}}_t$ is a vector of size R containing the graph frequency coefficients.

We can then define the diagonal filtering matrix $\mathbf{H}$, and fill it in order to perform filtering on the graph. For lowpass filtering, $H_{i,i} = 0$ if $\lambda_i < \lambda_{LP}$ and 1 otherwise, while for highpass filtering, $H_{i,i} = 0$ if $\lambda_i > \lambda_{HP}$ and 1 otherwise. The filtered regional time courses are then retrieved as:

$$\mathbf{X}_{\text{filt}} = \mathbf{V}\mathbf{H}\mathbf{V}^\top\mathbf{X}. \tag{2}$$

Lowpass and highpass filtering respectively yield the *aligned* and *liberal* subparts of the original functional signals [7], and depend on the selection of the filtering parameter, as more stringent filtering will retain a narrower graph frequency band. Here, we compute the average power spectral density (PSD) of the signals across subjects as a function of graph frequency, and deem aligned/liberal the higher/lower eigenvalue components that tally to P_{PSD}% of the PSD.

2.3. Brain/behaviour relationships

From the processed time courses $\mathbf{X}_{\text{Al}}$ and $\mathbf{X}_{\text{Lib}}$, we considered three metrics to characterise each region $r \in [1, 2, ..., R]$:

- The average alignment or liberality strength along time, akin to [7] and [9].
- The standard deviation of these same quantities along time.
- Their instantaneous change, which we quantified as $\frac{1}{T-1}\sum_{t=1}^{T-1}\frac{|X(r,t+1)-X(r,t)|}{2}$.

The last two metrics are inspired from the dynamic functional connectivity work of [14]. We used the Scikit-learn toolbox [15] to implement a nested cross-validation scheme in which an elastic net regression strategy was deployed. We used 3-fold cross-validation for the inner loop, and 2-fold cross-validation for the outer loop, and probed parameter ranges $\alpha = [0.25, 0.5, 0.75, 1, 1.5, 2]$ and $R_\ell = [0.01, 0.2, 0.4, 0.6, 0.8, 1]$. Here, α controls the extent of regularisation ($\alpha = 1$ indicates balanced data fitting and regularisation terms), while $R_\ell \in [0, 1]$ controls the ratio between ℓ_1 and ℓ_2 regularisation terms (a value of 0 amounts to ℓ_2 regularisation). The R^2 coefficient of determination was used as a quality metric.

For prediction accuracies with $R^2 > 0$, we went back to the full subject population, and fitted an elastic net model using optimal parameter values. We compared the resulting R^2 value to a null distribution computed non-parametrically. Because we conducted 96 such tests, we assessed significance at $\alpha = 0.0005$.

3. RESULTS

Prediction quality for the assessed metrics and range of P_{PSD} values is displayed in Figure 1. In total, only 10.13% of R^2 values exceeded 0, which indicates that in the majority of cases, prediction accuracy is very unsatisfying (worse than when using the mean of all data points).

Some behavioural domains could be predicted well regardless of the stringency in defining the aligned/liberal contributions (*i.e.*, for any P_{PSD} value), such as *Strength* (with standard deviation of liberality); in other cases, a low or a high P_{PSD} value was required (respective examples include *Depression*—instantaneous change of alignment—and *Working Memory (Bad)*—standard deviation of liberality).

On the best case across P_{PSD} values for each behaviour and metric, significance was reached for 7/17/13 behavioural scores for mean/standard deviation/instantaneous change of alignment, and 15/14/9 for liberality. In Figure 2, we plot the best nested cross-validation R^2 values for each behaviour, as well as matching R^2 coefficients recomputed on the whole subject population. We also display the type of metric that yielded this best case. It can be seen that alignment and liberality each contribute to some of the optimal predictions, while standard deviation dominates over mean and instantaneous change.

4. DISCUSSION AND CONCLUSION

In this work, we compared a set of GSP metrics in terms of predicting a broad range of behavioural variables. We observed that successful prediction could be achieved across di-

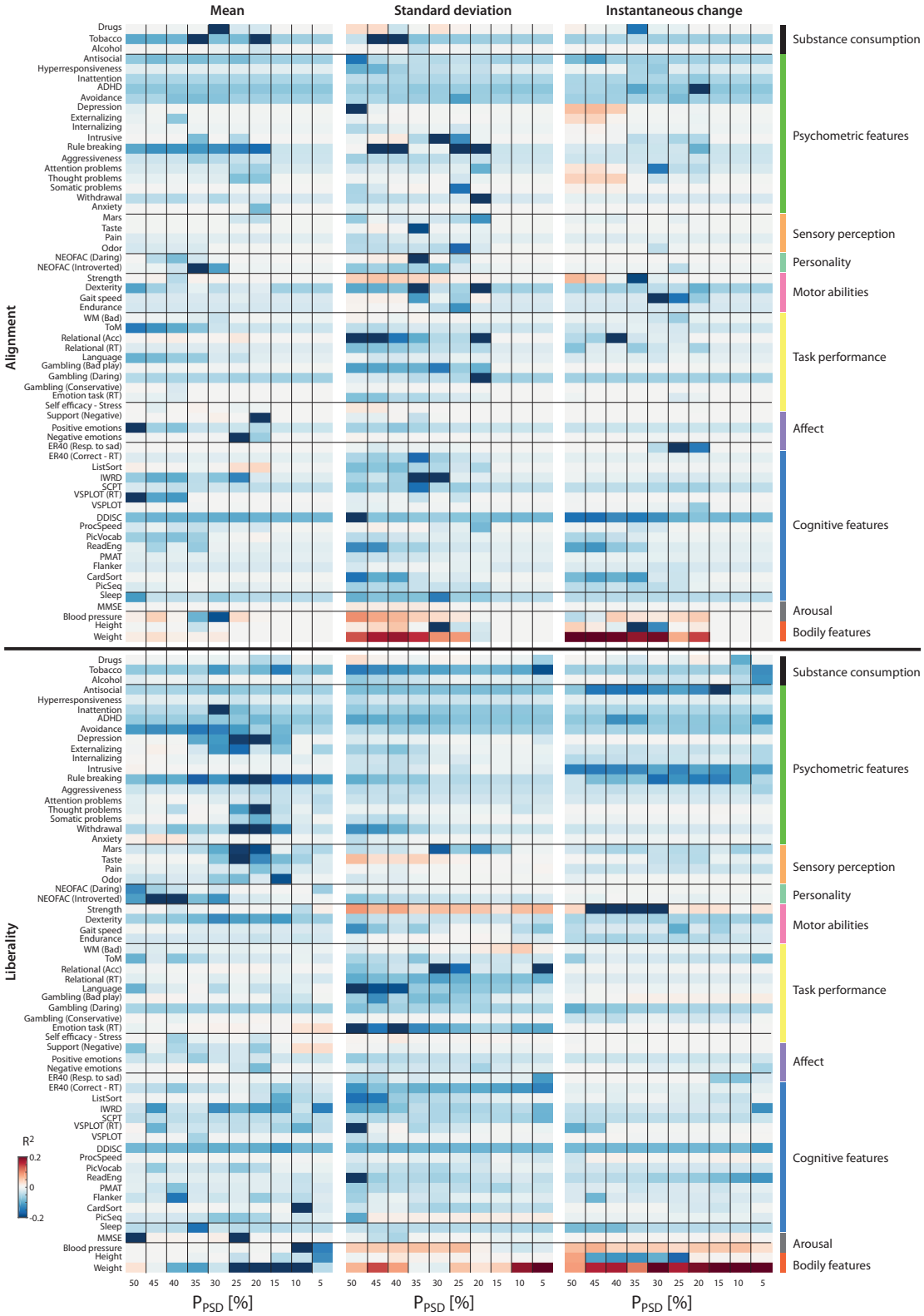

Fig. 1. **Significance of brain/behaviour relationships.** Across all 62 behavioural domains and investigated P_{PSD} values, R^2 coefficient obtained upon nested cross-validation.

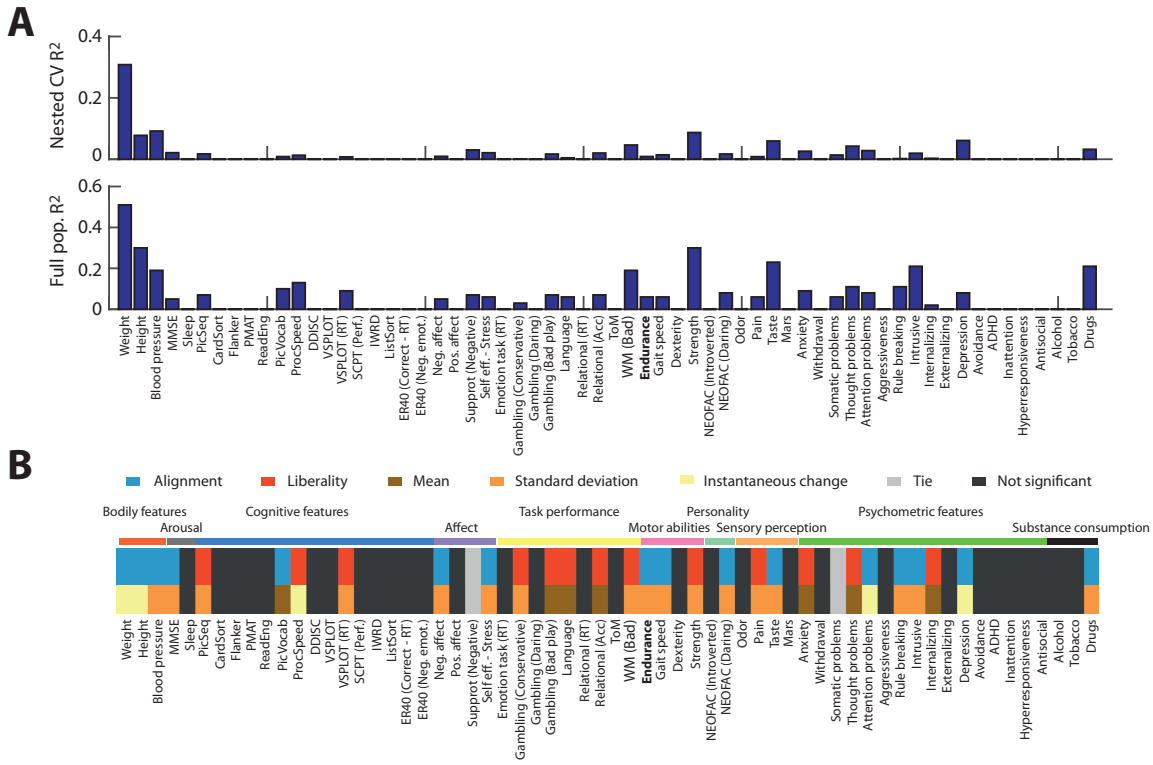

Fig. 2. **Comparison of metrics predictive potential.** **(A)** R^2 coefficients for all 62 behavioural domains in the best case scenario, when computed in nested cross-validation fashion (top) or back to the full dataset (bottom). **(B)** For each behavioural domain, the type of metric (alignment versus liberality, and mean versus standard deviation versus instantaneous change) that yielded the best prediction accuracy is colour coded.

verse functional domains, such as sensory perception, motor abilities, cognitive skills or arousal. Alignment and liberality had already been examined in previous work [7] when quantified as temporal averages; the present analyses confirm the relevance of the two metrics.

Our major finding is that beyond the use of a static measure, dynamic GSP metrics (whose use had been suggested in [8] without being practically applied) also contain relevant information: in several cases, the standard deviation or instantaneous change of alignment or liberality actually enabled significant prediction accuracies when it was not the case using static measures (see for example the *Strength* score in Figure 1).

There is an increasing understanding that the brain transits between moments of extensive cross-network interactions (when functional connectivity strongly differs from the underlying structure), and moments of more modular and structurally-conform activity [16, 17]. Dynamic GSP metrics likely capture such transitions as temporal reconfigurations of alignment and/or liberality.

An essential aspect is the definition of what an aligned or a liberal component is: so far, either a fixed number of eigenmodes was considered [7], or a median split of the PSD was used [9]. Our results show that in some cases, predictive potential is insensitive to this parameter choice, whereas in others, it is necessary to include a sufficient amount of eigenmodes (that is, use larger P_{PSD} values), probably because the meaningful structural interplays for the behaviours at hand are then embedded in more intermediate frequency eigenmodes. It is possible that the rarer occurrence of the opposite (better prediction as less eigenmodes are considered) was partly due to the ability of the elastic net approach to suppress irrelevant features by ℓ_1 regularisation; further examination using other regression strategies will help clarify this point.

An interesting perspective for future work will be to assess to what extent the observed effects exist at the whole-brain level, or at a spatially finer mesoscale. Practically speaking, one could for instance envision the derivation of *Slepian vectors*, which are linearly recombined eigenmodes with maximised concentration in a user-defined subset of nodes [18]. It would then become possible to investigate alignment and liberality at the level of individual networks, and thus further refine our understanding of human cognition.

5. REFERENCES

[1] A. Fornito, A. Zalesky, and M. Breakspear, "The connectomics of brain disorders," *Nature Reviews Neuroscience*, vol. 16, no. 3, pp. 159, 2015.

[2] B. T. Yeo, F. M. Krienen, J. Sepulcre, M. R. Sabuncu, D. Lashkari, M. Hollinshead, J. L. Roffman, J. W. Smoller, L. Zöllei, J. R. Polimeni, et al., "The organization of the human cerebral cortex estimated by intrinsic functional connectivity," *Journal of Neurophysiology*, vol. 106, no. 3, pp. 1125–1165, 2011.

[3] C. Caballero-Gaudes and R. C. Reynolds, "Methods for cleaning the BOLD fMRI signal," *NeuroImage*, vol. 154, no. December 2016, pp. 128–149, 2017.

[4] S. M. Plis, M. F. Amin, A. Chekroud, D. Hjelm, E. Damaraju, H. J. Lee, J. R. Bustillo, K. Cho, G. D. Pearlson, and V. D. Calhoun, "Reading the (functional) writing on the (structural) wall: Multimodal fusion of brain structure and function via a deep neural network based translation approach reveals novel impairments in schizophrenia," *NeuroImage*, vol. 181, pp. 734–747, 2018.

[5] T. A. Bolton, Y. Farouj, M. Inan, and D. Van De Ville, "Structurally-informed deconvolution of functional magnetic resonance imaging data," in *2019 IEEE 16th International Symposium on Biomedical Imaging (ISBI 2019)*. IEEE, 2019, pp. 1545–1549.

[6] D. I. Shuman, S. K. Narang, P. Frossard, A. Ortega, and P. Vandergheynst, "The emerging field of signal processing on graphs: Extending high-dimensional data analysis to networks and other irregular domains," *IEEE Signal Processing Magazine*, vol. 30, no. 3, pp. 83–98, 2013.

[7] J. D. Medaglia, W. Huang, E. A. Karuza, A. Kelka, S. L. Thompson-Schill, A. Ribeiro, and D. S. Bassett, "Functional alignment with anatomical networks is associated with cognitive flexibility," *Nat. Hum. Behav.*, vol. (in press), 2017.

[8] W. Huang, T. A. Bolton, J. D. Medaglia, D. S. Bassett, A. Ribeiro, and D. Van De Ville, "A Graph Signal Processing Perspective on Functional Brain Imaging," *Proceedings of the IEEE*, 2018.

[9] M. G. Preti and D. Van De Ville, "Decoupling of brain function from structure reveals regional behavioral specialization in humans," *arXiv preprint arXiv:1905.07813*, 2019.

[10] M. G. Preti, T. A. Bolton, and D. Van De Ville, "The dynamic functional connectome: State-of-the-art and perspectives," *NeuroImage*, vol. 160, no. December 2016, pp. 41–54, 2017.

[11] D. C. Van Essen, S. M. Smith, D. M. Barch, T. E. Behrens, E. Yacoub, and K. Ugurbil, "The WU-Minn Human Connectome Project: An overview," *NeuroImage*, vol. 80, pp. 62–79, 2013.

[12] J. Tournier, F. Calamante, A. Connelly, et al., "MRtrix: diffusion tractography in crossing fiber regions," *International Journal of Imaging Systems and Technology*, vol. 22, no. 1, pp. 53–66, 2012.

[13] M. F. Glasser, T. S. Coalson, E. C. Robinson, C. D. Hacker, J. Harwell, E. Yacoub, K. Ugurbil, J. Andersson, C. F. Beckmann, M. Jenkinson, et al., "A multimodal parcellation of human cerebral cortex," *Nature*, vol. 536, no. 7615, pp. 171–178, 2016.

[14] J. Liu, X. Liao, M. Xia, and Y. He, "Chronnectome fingerprinting: identifying individuals and predicting higher cognitive functions using dynamic brain connectivity patterns," *Human brain mapping*, vol. 39, no. 2, pp. 902–915, 2018.

[15] F. Pedregosa, G. Varoquaux, A. Gramfort, V. Michel, B. Thirion, O. Grisel, M. Blondel, P. Prettenhofer, R. Weiss, V. Dubourg, et al., "Scikit-learn: Machine learning in python," *Journal of machine learning research*, vol. 12, no. Oct, pp. 2825–2830, 2011.

[16] R. F. Betzel, M. Fukushima, Y. He, X.-n. Zuo, and O. Sporns, "Dynamic fluctuations coincide with periods of high and low modularity in resting-state functional brain networks," *NeuroImage*, vol. 127, pp. 287–297, feb 2016.

[17] M. Fukushima, R. F. Betzel, Y. He, M. P. van den Heuvel, X.-N. Zuo, and O. Sporns, "Structure–function relationships during segregated and integrated network states of human brain functional connectivity," *Brain Structure and Function*, vol. 223, no. 3, pp. 1091–1106, 2018.

[18] M. Petrovic, T. A. Bolton, M. G. Preti, R. Liégeois, and D. Van De Ville, "Guided graph spectral embedding: Application to the C. elegans connectome," *Network Neuroscience*, vol. 3, no. 3, pp. 807–826, 2019.